

PAPER • OPEN ACCESS

## Analysis of Dynamic Interactions between Different Drivetrain Components with a Detailed Wind Turbine Model

To cite this article: A Bartschat *et al* 2016 *J. Phys.: Conf. Ser.* **753** 082022

View the [article online](#) for updates and enhancements.

### Related content

- [Research of dynamic loading in a drivetrain by means of mathematical modeling](#)  
N S Sokolov-Dobrev, M V Ljashenko, V V Shekhovtsov et al.
- [Study on Active Suppression Control of Drivetrain Oscillations in an Electric Vehicle](#)  
Lei Huang and Ying Cui
- [Adaptive Third-Order Leader-Following Consensus of Nonlinear Multi-agent Systems with Perturbations](#)  
Sun Mei, Chen Ying, Cao Long et al.

# Analysis of Dynamic Interactions between Different Drivetrain Components with a Detailed Wind Turbine Model

A Bartschat<sup>1</sup>, M Morisse<sup>2</sup>, A Mertens<sup>2</sup>, J Wenske<sup>1</sup>

<sup>1</sup>Fraunhofer Institute for Wind Energy and Energy System Technology, IWES, Hannover, Germany

<sup>2</sup>Institute for Drive Systems and Power Electronics, Leibniz Universität Hannover, Hannover, Germany

E-Mail: Arne.Bartschat@iwes.fraunhofer.de

**Abstract.** The presented work describes a detailed analysis of the dynamic interactions among mechanical and electrical drivetrain components of a modern wind turbine under the influence of parameter variations, different control mechanisms and transient excitations. For this study, a detailed model of a 2MW wind turbine with a gearbox, a permanent magnet synchronous generator and a full power converter has been developed which considers all relevant characteristics of the mechanical and electrical subsystems. This model includes an accurate representation of the aerodynamics and the mechanical properties of the rotor and the complete mechanical drivetrain. Furthermore, a detailed electrical modelling of the generator, the full scale power converter with discrete switching devices, its filters, the transformer and the grid as well as the control structure is considered. The analysis shows that, considering control measures based on active torsional damping, interactions between mechanical and electrical subsystems can significantly affect the loads and thus the individual lifetime of the components.

## 1. Introduction

As the size and the rated power of modern wind turbines are increasing, also the loads on the components are increasing exponentially. Higher loads and the need for reducing the costs to ensure the competitiveness with conventional and other renewable energy sources are challenges for wind turbine manufacturers and the suppliers. In addition, manufacturers and operators of wind turbines are still facing unexpected failures of various components which affect the overall reliability and causes unscheduled downtime as well as cost intensive maintenance. In the electrical subsystem of a wind turbine, the power converters are a common source of failure [1]. In addition, the gearbox, the pitch-system and the generator are also among the components with high failure rates ([2], [3]). Considering the costs and downtime caused by failures of such components, bearing damages in gearboxes and IGBT (insulated gate bipolar transistor) blasts in power converters are particularly critical. However, the causes and mechanisms underlying these failures are mostly unknown today. Among the potential causes are the highly dynamic interactions of aerodynamic, mechanical and electrical turbine subsystems which might not be covered in sufficient detail by the models underlying today's design procedures. However, some fundamental interactions between these subsystems are taken into account for the control of the wind turbine like the torque control of the generator for variable-speed operation for obtaining the maximum aerodynamic efficiency of the wind turbine. In addition, active torsional damping (ATD) is a widely applied counter measure for reducing torsional vibrations of the mechanical drivetrain and decreasing the stresses on the components to extend their individual lifetime [4]. The conventional approach of active torsional damping is based on band-pass filters (BPF) for the



detection of torsional vibrations and a dynamic torque control of the generator. In this approach, the generator inserts additional dynamic torque into the drivetrain and therefore the power converter has to deal with an increase of dynamic loads.

In order to analyse these dynamic interactions using a detailed wind turbine model, this paper investigates the influences of active torsional damping on the thermal stress and resulting lifetime consumption of an IGBT-based power converter. The article is structured as follows: In Section 2, a detailed model covering the aerodynamic, mechanical and electrical parts of a modern 2MW wind turbine is described. In Section 3, the approach of the simulations and the results are presented and discussed. Finally, conclusions from the findings and an outlook are given in Section 4.

## 2. Detailed wind turbine model

Many researches concerning the dynamic properties and behaviour of modern wind turbines are focused on only one particular subsystem. The depth of modelling is depending on the focus of the simulation approach to minimize the calculating time of the model. Studies concerning the modelling of the electrical subsystem, like the power converter, often neglect the influence of the mechanical and aerodynamic subsystems on the overall dynamic behaviour of the complete wind turbine. Usually this is carried out by using a simplified power curve approach and a simplified low-order torsionally elastic model for aerodynamic and mechanical calculations ([5], [6]). Various studies showed the differences between calculating the aerodynamic torque with a power curve approach and using the blade element momentum theory (BEM) in addition with structural dynamic models of the rotor ([7], [8]). These studies have shown that models which are too simplified often neglect important dynamic properties of the wind turbine. Therefore, this implies that results regarding controller set-ups, overall system dynamics or power quality studies, obtained on the basis of such models, are not sufficient.

Load calculations are often carried out by means of tools like BLADED, which offer very detailed aeroelastic calculations in combination with a low-order torsionally elastic representation of the drive train. However, the electrical properties of a modern wind turbine are not covered in sufficient detail. Therefore, studies regarding the dynamic interactions have to be carried out using other tools and models. Analyses on load reducing controllers such as ATD or individual blade pitch control need to have detailed models to achieve accurate results. For example in [9], two different ATD methods are analysed by using the NREL software FAST for aerodynamic calculations and MATLAB/Simulink for the mechanical and electrical subsystems of the model.

As ATD is a widely analysed and simple to implement method for the mitigation of loads of the drivetrain, such control structures are applied in the power converters of modern wind turbines. In order to observe the loads of the power converter, which has to deal with higher dynamics in the case of ATD, a detailed model is used in the study presented in this paper.

To achieve a better understanding of the component interactions and the loads of different drivetrain components, a detailed 2MW wind turbine model was developed using MATLAB/Simulink for the control structures, the mechanical parts and the aerodynamic calculations and PLECS for the electrical subsystems. This set-up allows the simulation to be carried out in one simulation environment which is a benefit in terms of performance and customizability. In addition this set-up enables to simulate the complete dynamic response of wind turbines combining the aeroelastic, mechanical and electrical subsystems. The structure of the complete model including the energy conversion chain from the kinetic energy of the wind to the electrical energy being fed into the power-grid is shown in Figure 1. The overall parameters of the wind turbine are chosen to ensure a typical 2 MW system configuration. These parameters are listed in Table 1.

The presented model covers a fully coupled aeroelastic rotor model, a detailed torsionally elastic drivetrain as well as an electrical subsystem with a 2 MW permanent magnet synchronous generator (PMSG) and a fully rated power converter. A more detailed description of the aeroelastic, the mechanical and of the electrical subsystems of this model is given in the following sections.

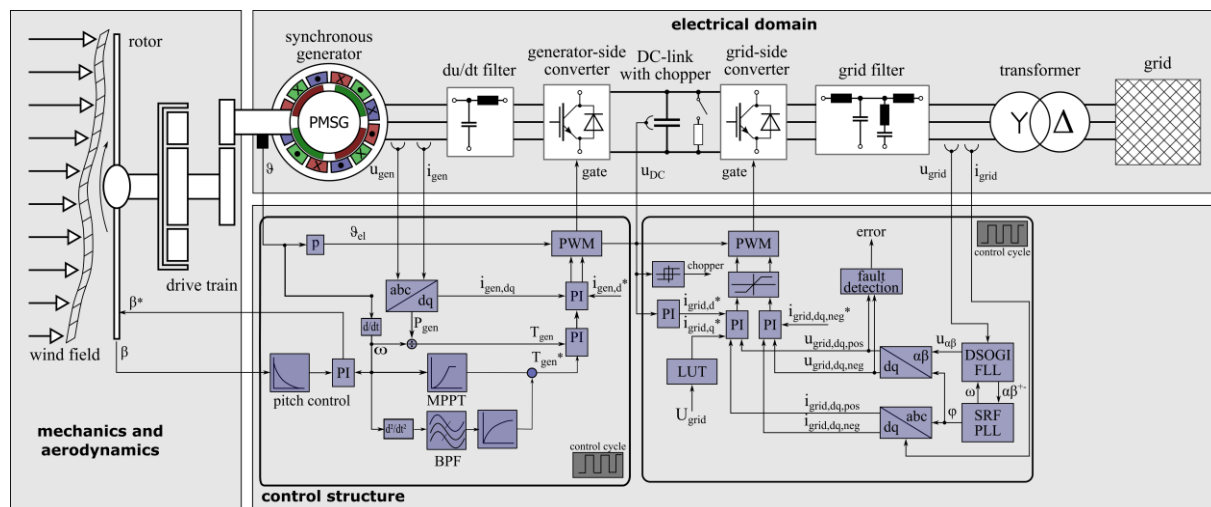


**Figure 1.** Structure of the detailed 2MW wind turbine model with PMSG and fully rated power converter

**Table 1.** Substantial system parameters of the 2 MW wind turbine model

System parameters		Electrical parameters	
Rated rotor power	2.22 MW	Rated electrical power	2 MW
Rated wind speed	10.8 m/s	Rated generator power	2.2 MW
Optimal tip-speed ratio	6.8	Rated voltage	690 V
Maximum power coefficient	0.46	Rated current	1.86 kA
Rotor speed range	4.8-15.2 rpm	Converter switching frequency	2.5 kHz
Rotor diameter	90 m	Converter DC-link voltage	1.1 kV
Gear ratio	1:119.84	Rated generator speed	1800 rpm
Overall system efficiency	90%	Number of pole pairs	2

### 2.1. Aerodynamic and mechanical subsystem

Figure 2 shows the structure of the aerodynamic and the mechanical subsystems of the model. The aerodynamic model is based on an unsteady blade-element momentum theory (BEM) and covers an implementation of rotational sampling, turbulent wind fields and a tower model for the characteristic tower dam excitations and for the structural dynamics. A proper implementation of the possible excitations such as turbulence and especially the tower dam effect is crucial for analysing the overall dynamic behaviour of a wind turbine. Therefore these effects are implemented in the model based on the work described in [10]. The mechanical characteristics of the rotor blades are covered by a dynamic beam theory approach which takes into account the first two flapwise and the first edgewise natural frequencies and their mode shapes. The aeroelastic calculations are fully coupled in order to achieve a proper representation of the dynamic behaviour of the rotor (see Figure 2). The solutions of the aeroelastic calculations are verified using FAST v8 and they are showing a very good agreement in terms of the dynamic response and accuracy. The structural and the aerodynamic properties of the rotor blades used in this model are derived from the well-known NREL 5 MW offshore turbine and scaled to match 2 MW characteristics [11].

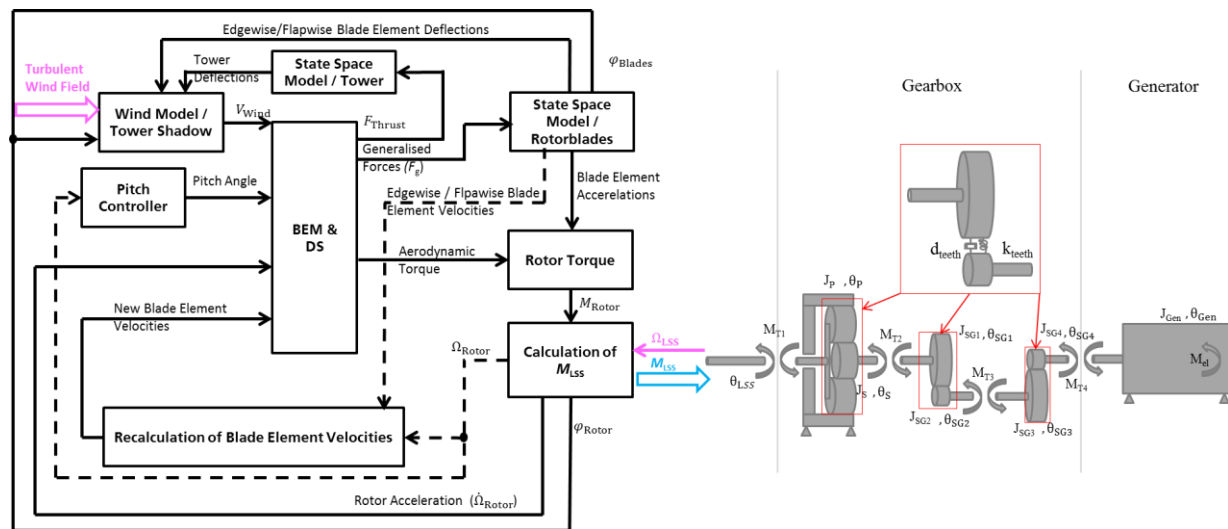


**Figure 2.** Structure of the aerodynamic and mechanical subsystems of the wind turbine model

In addition to the aeroelastic subsystem, the model covers a detailed torsionally elastic drivetrain with eight masses and gearbox characteristics such as time-varying meshing stiffness as well as backlash to match the characteristics of a typical three-stage gear (one planetary and two parallel stages). This approach ensures that the drivetrain model covers a wide range of realistic natural frequencies as well as different modes of excitations which can affect the dynamic response of the whole wind turbine model. In addition, the consideration of different modes of excitations of the mechanical drivetrain leads to a more realistic analysis of the influences of ATD because the overall dynamic response is captured in greater detail. To achieve a realistic representation of the drivetrain dynamics the parameters of the mechanical drivetrain are derived from finite element models as well as from comparable models described in the literature [12]. The complete aeroelastic and mechanical subsystems of the model cover the natural frequencies listed in Table 2.

**Table 2.** Natural frequencies of the mechanical parts of the modelled wind turbine

Mode	Natural frequency (Hz)	Mode	Natural frequency (Hz)
1 (1.Tower)	0.386	7 (2.Drivetrain)	57.73
2 (1.Blade flapwise)	0.959	8 (3.Drivetrain)	132.67
3 (1.Drivetrain)	2.55	9 (4.Drivetrain)	209.57
4 (2.Tower)	2.675	10 (5.Drivetrain)	330.79
5 (1.Blade edgewise)	2.713	11 (6.Drivetrain)	514.56
6 (2.Blade flapwise)	3.152	12 (7.Drivetrain)	3086

Due to the implementation of effects like tower dam, variable meshing stiffness as well as the shape function for a realistic representation of the back emf (electromagnetic force) (see Section 2.2), the diagram in Figure 3 shows that the probability to induce vibrations in variable speed operation of the modeled wind turbine is very high. Table 2 shows that the natural frequencies of the mechanical drivetrain can reach high values. This is a benefit of this model because the electrical subsystem is modeled in detail containing high frequent modes of excitations as well. Therefore the model is able to accurately simulate the dynamic response of the complete wind turbine and the interactions of the different subsystems.

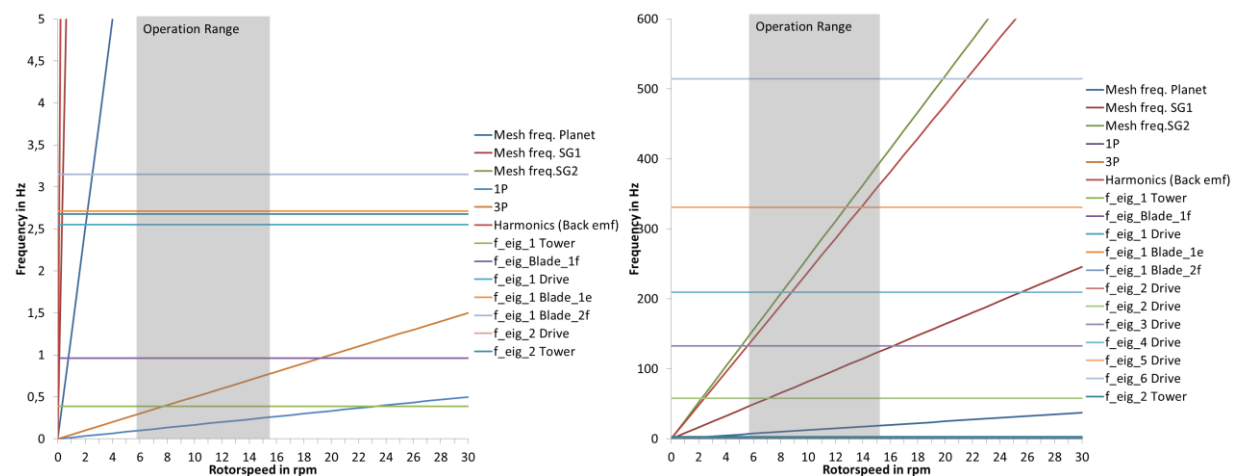


**Figure 3.** Natural frequencies and excitations of the aeroelastic and mechanical subsystem of the modelled wind turbine (frequencies up to 5 Hz on the left side and frequencies up to 600 Hz on the right side)

From the analysis, the operation at speeds around 8 and 13 rpm suggest that induced vibrations due to the variable meshing stiffness of the drivetrain model and the shape function of the back emf are very likely to occur. Normally the drivetrain would be designed in a way to minimize such critical operating conditions because induced vibrations can provoke higher loads on mechanical drive train parts like bearings and pinions. Considering the harmonics of the different excitation would lead to even more intersections in the diagram shown in Figure 3. Even though, the dynamic excitations can be only minimized and not completely avoided in the design process and in the variable speed operation of modern wind turbines. Therefore, it is important to consider these excitations when analysing the effects of active torsional damping.

## 2.2. Electrical subsystem

The electrical model consists of a permanent-magnet synchronous generator (PMSG) based on the T-equivalent circuit diagram in the rotor-reference dq-frame and a fundamental wave model, as well as a shape function for the back emf presented in [13]. This ensures a realistic coupling between the mechanical and the electrical subsystem in the air gap of the generator and a possible source of dynamic excitations of the drivetrain.

The generator-side and the grid-side converter are both two-level IGBT converters with three parallel modules for each half bridge. Their forward characteristic as well as their thermal behaviour is extracted from the datasheet of an IGBT module which is widely used in wind applications [14]. In addition, the power-electronic devices are modeled as discrete components considering the actual switching states of the single semiconductors. Because the lifetime of semiconductors is calculated by means of their thermal stress, a similar approach is used in this study. In order to estimate the lifetime consumption the junction temperature of the IGBT is used [15]. The junction temperature is the indicator for the thermal stress of a switching device regarding the thermal expansion of the material due to the thermal cycles. However, only failure mechanisms concerning the thermal load can be taken into account in this way.

During the simulation, the conduction and the switching power losses are calculated in every time step. The losses of the switching devices are used as an input for the thermal model of the half bridge whose thermal data are derived from the same data sheet. The results of the thermal model are the temperature swings of the junction temperature of the switching devices. After the simulation these values are post-processed by means of a rainflow algorithm followed by an estimation of the lifetime consumption based on an experimentally validated power cycling analysis from the LESIT project ([16], [17]). As there are some restrictions based on the differences in the experiment which was used

to validate the model of the lifetime calculation and the simulation performed in this study, the results should not be interpreted as absolute values. However, the results can be used to qualitatively assess the differences between different simulation scenarios, parameter configurations and control strategies.

In addition to the detailed model of the power converter, the model covers a triple-wound transformer as well as filters to fulfil the requirements of the grid connection.

### *2.3. Control structure*

The control structure implemented in the model is shown in Figure 1. The structure consists of the usual control strategy of a typical wind turbine like torque control for variable-speed operation and pitch control for reducing the power above rated wind speed. The model uses a PI controller with gain scheduling for the pitch to limit the rotational speed above rated wind speed. Below rated wind speed the PMSG is controlled by a torque control whose reference value is calculated by a maximum power point characteristic to enable variable speed operation. The torque is used as the reference value for the current control of the rotor-side power converter. The grid-side power converter controls the DC-link voltage and the reactive current component fed into the grid. In addition, ATD can be added to the torque control structure (e.g. [18]). This option enables additional active damping of several natural frequencies of the drivetrain and thus a load reduction for the mechanical parts. For this purpose, the acceleration signal of the rotor of the generator is processed by band-pass filters tuned for three different natural frequencies of the drivetrain. The filtered signals are processed through low-pass filters which produce torque signals as their outputs. These signals are added to the reference value of the torque controller. As ATD is a common measure to lower loads in the mechanical drivetrain, it is important to consider this control structure when analysing the interactions between mechanical and electrical subsystems.

## **3. Results and discussion**

In order to analyse the dynamic interactions between the electrical and the mechanical subsystems of the wind turbine in detail, an investigation on the impact of ATD on the loads of the power converter is carried out. Previous research has demonstrated that ATD can extend the lifetime of the drivetrain in wind turbine applications due to the load reduction [18]. But as the demand of dynamic torque of the generator rises, the power converter will have to deal with more dynamic currents and hence more dynamic loads. To examine the dynamic interactions of the power converter with the mechanical drivetrain two simple simulation cases are used. These are presented in the following sections.

### *3.1. Steady wind condition*

The first simulation scenario covers 40s of steady-state wind condition below rated wind speed ( $v = 9.8$  m/s) and a symmetric three-phase voltage drop by 80% at  $t = 20$ s which causes a transient excitation of the system due to the lower torque of the generator. In order to take into account different drivetrain properties, four different parameter configurations for the stiffness values of the four shafts in the drivetrain model (see also Figure 2) are considered in the first analysis (see Table 3). The variation of these parameters leads to changes of the natural frequencies and the overall dynamic properties of the drivetrain. Therefore, this analysis is able to show how the design of the mechanical drivetrain components can affect the loads in the electrical subsystems like the power converter. The first configuration is the base setup with the properties mentioned in Table 2 and Figure 3. Configurations No. 2 to No. 4 are derived from the first one but with changed parameters for the stiffness values of the four shafts (see also Table 3). As the natural frequencies of the drivetrain are varying in the four simulation scenarios, the configuration of the ATD is adapted accordingly in these scenarios.

**Table 3.** Variation of the stiffness values of the four shafts (see Figure 2) and ATD-damped frequencies for the four configurations

Configuration	$k_{S1}$ [pu]	$k_{S2}$ [pu]	$k_{S3}$ [pu]	$k_{S4}$ [pu]	$f_{1\_ATD}$ [Hz]	$f_{2\_ATD}$ [Hz]	$f_{3\_ATD}$ [Hz]
No. 1	1	1	1	1	2.55	57.73	330.79
No. 2	1	1	0.7	0.9	2.55	54.95	329.68
No. 3	0.8	0.8	1	0.09	2.16	18.83	205.99
No. 4	1	1	1	10	2.57	126.9	365.09

The simulation results of configuration No. 1 in Figure 4 are showing that the ATD approach is able to reduce torsional vibrations in the drivetrain. The amplitudes of the lowest frequencies damped by ATD are reduced by a factor of approximately two compared to the undamped results. Even the highest frequency (330.79 Hz) shows a small reduction in the amplitude due to the fast dynamics of the torque control of the PMSG. This will lead to reduction of the fatigue loads of the mechanical drivetrain and therefore extend the expected lifetime. However, as already mentioned, more dynamic torque for the purpose of drivetrain damping, leads to an increase in dynamic currents in the power converter. Due to the conduction and switching losses, the thermal loads of the switching devices are increased as well.

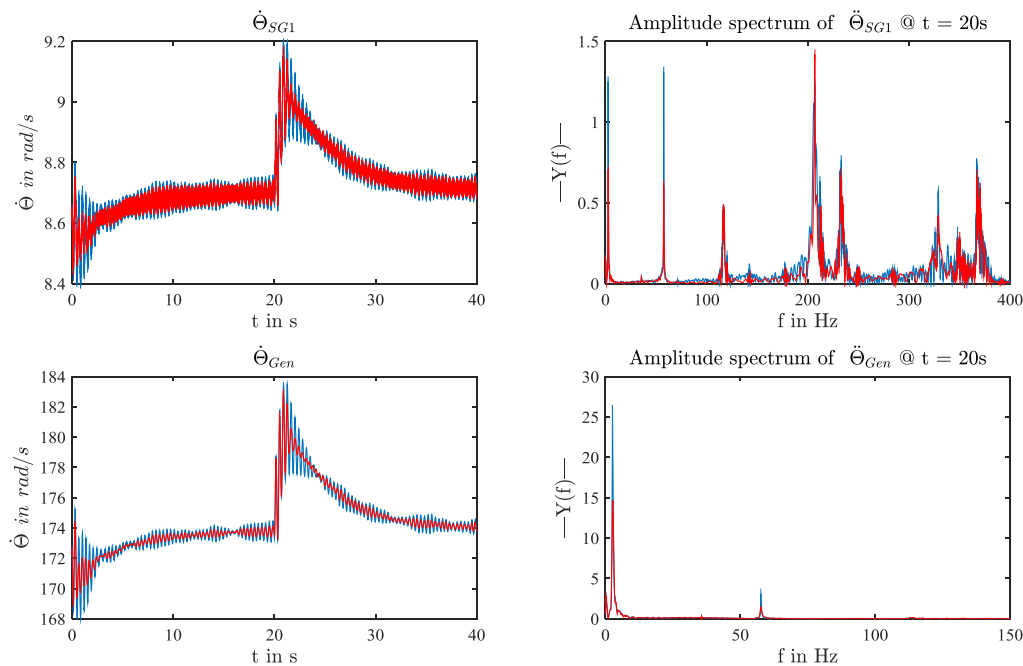


**Figure 4.** Rotational speeds and amplitude spectrum of the first pinion of the first spur gear (SG1) (top) and the generator (Gen) (bottom) for the first simulation scenario and configuration No. 1; red lines are with activated ATD, blue lines are without ATD

Figure 5 shows the impact of the ATD on the lifetime consumption of an IGBT in the power converter of the model for configuration No.1.



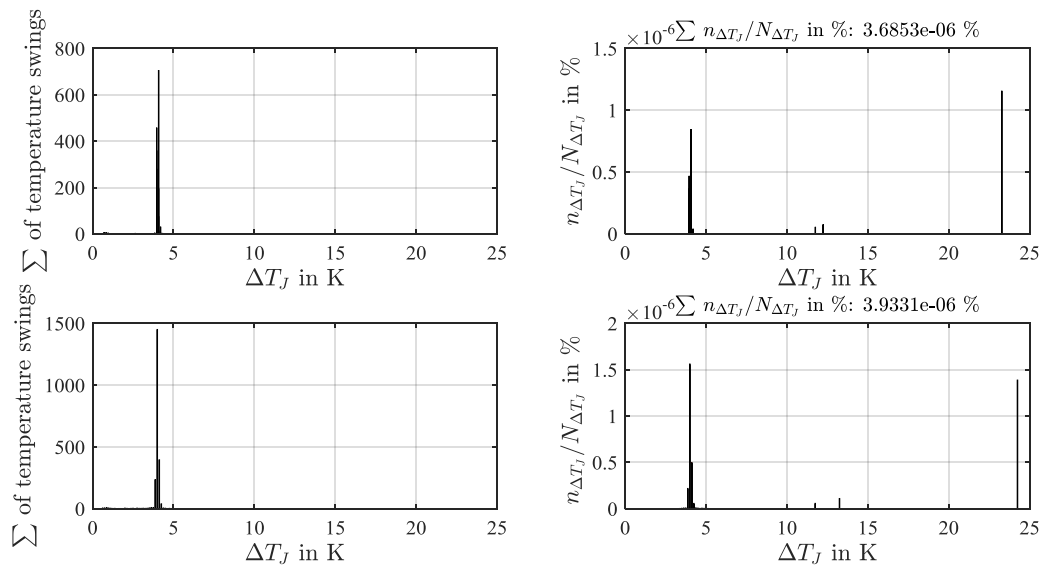


**Figure 5.** Temperature swings and lifetime consumption of an IGBT in the power converter with ATD (bottom) and without ATD (top) for the first simulation scenario and configuration No.1

According to the results, ATD leads to a greater number of temperature swings of about 4 °K. In addition, the highest temperature swing is enlarged by approximately 1°K in the case of ATD. Despite the really low number of such high temperature swings, the contribution to the lifetime consumption is not negligible. These differences are leading to an increase of the overall lifetime consumption of about 6.72 % in the underlying simulation. The results of the four simulations are summed up in Table 4.

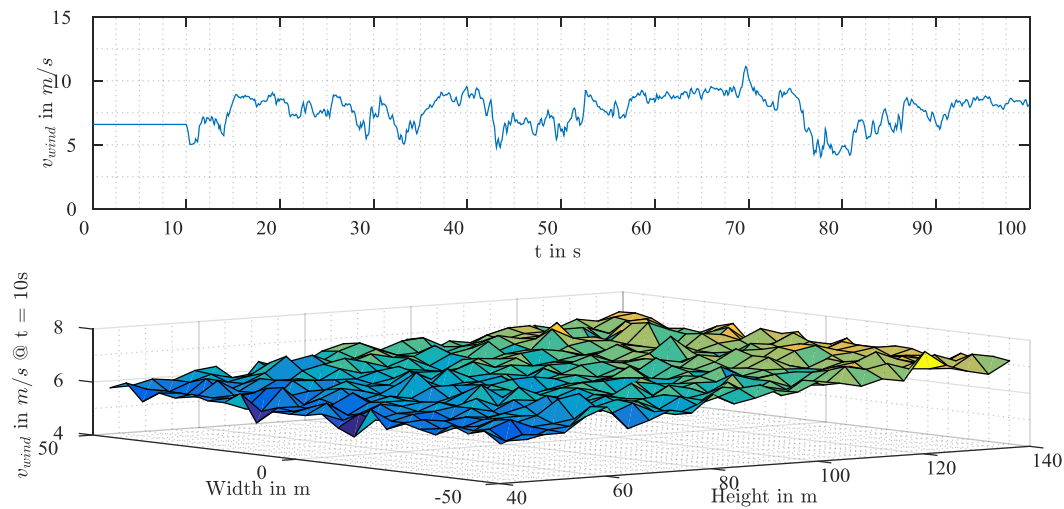
**Table 4.** Lifetime consumption of an IGBT in the power converter for the four drivetrain configurations under steady wind conditions

Configuration	Lifetime consumption without ATD in %	Lifetime consumption with ATD in %	Difference in %
No. 1	3.685E-06	3.933E-06	6.724
No. 2	3.681E-06	3.941E-06	7.052
No. 3	3.710E-06	4.241E-06	14.317
No. 4	3.679E-06	3.970E-06	7.896

As indicated in Table 4, the characteristics of the mechanical drivetrain can considerably affect the loads and with that the lifetime consumption of the power converter. Especially configuration No. 3, which simulates a more malleable drivetrain configuration with lower torsional natural frequencies, causes an increase in life time consumption of about 14 %.

### 3.2. Part-load and variable-speed operation

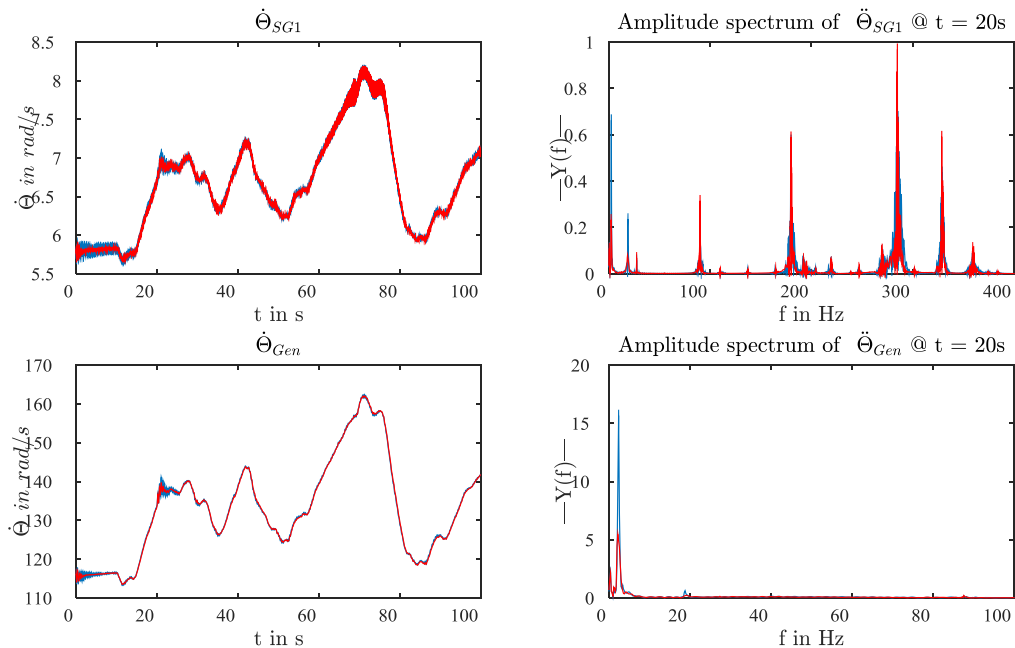
The second simulation scenario covers an analysis of the dynamic interactions of the mechanical and the electrical subsystem in part-load operation below rated wind speed with variable-speed operation due to unsteady wind conditions. This analysis shows how ATD can affect the operation in variable speed conditions where it is very likely that the occurrences of turbulence and variable meshing stiffness will cause some excitations to the system.



**Figure 6.** Wind speed for the simulation of part-load operation; average wind speed of the turbulent wind field over the simulation time (top) and an example of the turbulent wind field at  $t = 10$ s

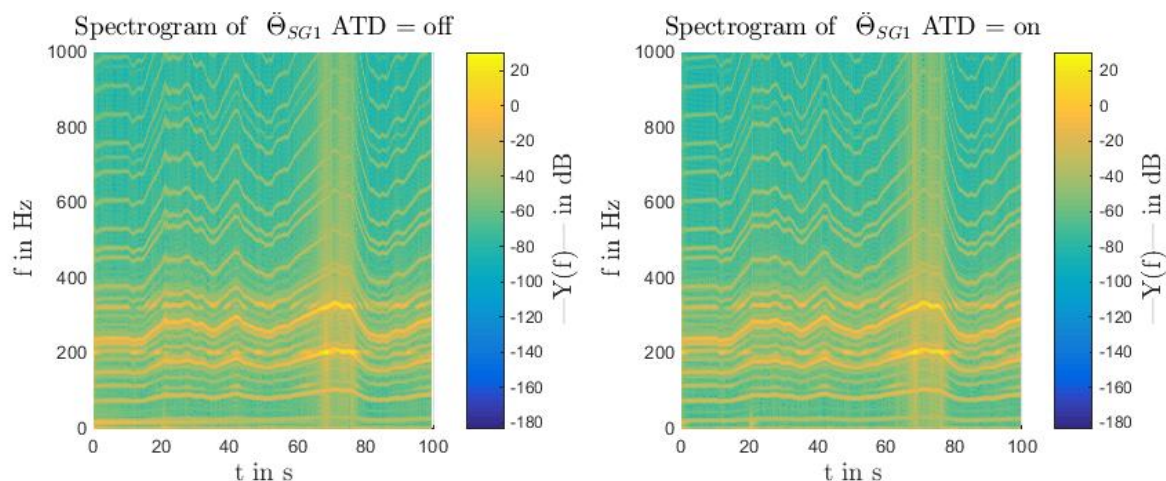
The simulation covers 100s of turbulent wind below rated wind speed. The first 10 seconds of the simulation are executed using steady wind conditions by means of non-variable mean wind speed at hub height in order to reduce the transient oscillation caused by the states of the integrators of the model. After 10 seconds the mean value of the wind field at hub height varies like it is shown in Figure 6. In the same way as in the simulations presented in Section 3.1, this scenario also covers an additional transient excitation by a symmetric 3-phase voltage drop by 80% at  $t = 20$ s. Due to the fact that the drivetrain configuration No. 3 showed the highest effect on the loads of the power converter, only this configuration is considered in the following analysis of the part-load operation.

Figure 7 shows the rotational speeds and amplitude spectrums of the corresponding accelerations of the generator and the first pinion of the first spur gear. The results reveal that ATD is able to reduce the low frequency torsional vibrations up to 20 Hz after a transient excitation and during the normal operation, which will cause a decrease in fatigue loads of the drivetrain but an increase in power converter loads. However, the implemented ATD approach is not able to reduce torsional vibrations with higher frequencies of above 50 Hz although one BPF is tuned for 205.99 Hz in this simulation. This effect is visible in the FFT-analysis results of the acceleration signals. Although surprising at the first glance, this observation is plausible because the drivetrain configuration No. 3 has a very malleable high speed shaft (HSS). Therefore, the acceleration signal for the ATD which is measured at the rotor of the generator does not contain any higher-frequency components.



**Figure 7.** Rotational speeds and amplitude spectra of the generator and the first pinion of the first spur gear for the second simulation scenario and configuration No. 3 with part-load operation; red lines are with activated ATD, blue lines are without ATD

The plot of the rotational speed of the first spur gear and the rotor of the generator lacks higher-frequency components. As mentioned before there are no vibrations with high frequencies at the rotor of the generator. In addition, Figure 8 shows that vibrations with approximate 330 Hz are induced in the gearbox at  $t = 70s$  due to the excitation with the variable meshing stiffness. However, the rotor of the generator is not showing these vibrations at all. Therefore, these vibrations with high frequencies are not transmitted to the generator and they have no effect on the ATD control.



**Figure 8:** Spectrogram of the acceleration of the first pinion of the first spur gear at variable-speed operation for configuration No. 3

By observing the power-converter IGBT lifetime consumption during the simulation with and without enabled active torsional damping in Figure 9, it is clear that ATD causes higher loads of the power converter of about 5.7 %, despite the fact that only the lowest frequencies are damped. The used

ATD approach is not able to detect vibrations of the drivetrain with higher frequencies in case of high speed shafts with low stiffness values. That leads to the conclusion that it is necessary to use additional signals and sensors or another approach like model-based observers to detect vibrations of the drivetrain.

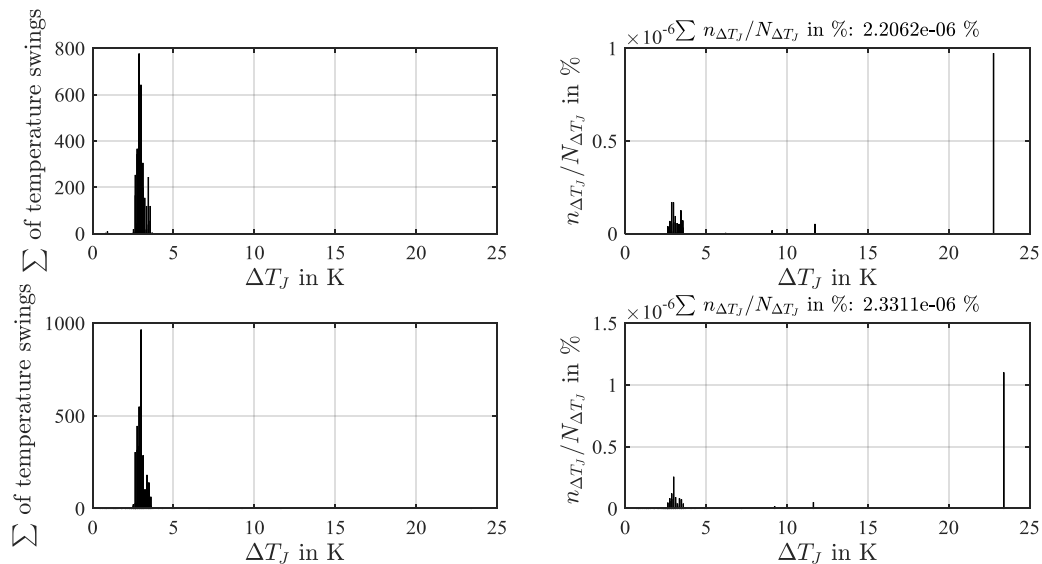


**Figure 9.** Temperature swings and lifetime consumption of an IGBT in the power converter with ATD (bottom) and without ATD (top) for the second simulation scenario and configuration No.3

#### 4. Conclusion and outlook

Detailed wind turbine models can be used to investigate the dynamic interactions between the mechanical and the electrical subsystems. This work shows that ATD is able to lower loads in the mechanical drive train but is also able to cause higher loads in the power converter. Therefore this paper investigates the interactions of those subsystems. The results in this paper are not able to represent the absolute lifetime consumption of a power converter for wind turbine applications, but they are a good way to show how control strategies and the design of mechanical drivetrain components can affect the dynamic interactions of mechanical and electrical subsystems.

The results show that the ATD approach in this investigation can significantly lower the loads in the mechanical drivetrain but at the same time causes higher loads in the electrical subsystem. The variation of parameters of the mechanical drivetrain reveals that the design process of the mechanical parts does not only affect the dynamic mechanical loads but also has an impact on the lifetime of a power converter with ATD. Therefore, it is necessary to take into account the dynamic interactions between mechanical and electrical subsystems of a modern wind turbine in order to improve the design process with respect to the reliability of the complete wind turbine. In order to produce results regarding the actual fatigue loads of different components using a detailed model based approach like presented in this paper, it is considered important to validate the modelling approach with measurements.

The investigation presented in this paper is based on a wind turbine model with a PMSG and a fully rated power converter. Another widely applied generator-converter topology in wind turbines is a doubly fed induction generator (DFIG) with partially rated converter. Because of the major differences between PMSG-based and DFIG-based turbines and their control strategy, the PMSG-specific results presented in this paper are not transferable without detailed analysis. An investigation of the dynamic interactions in case of a typical wind turbine with DFIG as well as the validation of the models is the subject of ongoing work.

## Acknowledgements

The present work was carried out within the Fraunhofer-Innovationscluster “Leistungselektronik für regenerative Energieversorgung” (Innovation Cluster on Power Electronics for Renewable Energy Supply). The project funding by the German Federal State of Lower Saxony by the initiative "Niedersächsisches Vorab" and by the Fraunhofer-Gesellschaft is gratefully acknowledged. The used wind velocity data is based on measured data from the offshore research platform FINO 1 and is funded by the German Federal Ministry for Economic Affairs and Energy BMWi and Projektträger Jülich.

## References

- [1] Fischer K 2015 Towards reliable power converters for wind turbines: field-data based identification of weak points and cost drivers *in Scientific Proceedings of EWEA, Paris, 17-20 November 2015*
- [2] Carrol J, McDonald A, McMillan D 2015 Failure rate, repair time and unscheduled O&M cost analysis of offshore wind turbines *Wind Energy* DOI: 10.1002/we.1887
- [3] Carrol J, McDonald A, McMillan D 2015 Reliability comparison of wind turbines with DFIG and PMG drivetrains *IEEE Transactions on Energy Conversion* vol. **30** pp 663-670
- [4] Licari J, Ugalde-Loo C, Ekanayake J, Jenkins N 2013 Damping of Torsional Vibrations in a Variable-Speed Wind Turbine *IEEE Transactions on Energy Conversion* vol. **28** pp 172-180
- [5] Bisoyi, S. K., Jarial, R. K., and Gupta, R. A., 2013 Modelling and control of variable speed wind turbine equipped with PMSG *Int. J. Emerg. Technol. Comput. Appl. Sci. IJETCAS* vol. **6**, pp. 56–62
- [6] Giaourakis D, and Safacas A. 2016 Quantitative and qualitative behaviour analysis of a DFIG wind energy conversion system by a wind gust and converter faults *Wind Energy*, vol. **19**, pp. 527–546.
- [7] Ramtharan, G, Caliao N, Bossanyi E, and Jenkins N, 2008 Modelling of aero and structural dynamics of wind turbines for power system studies *16th PSCC, Glasgow, Scotland*
- [8] Ramtharan, G, Bossanyi, E, Jenkins, N, 2007 Influence of Rotor Structural Dynamics Representations on the Electrical Transient Performance of FSIG and DFIG Wind Turbines *Wind Energy* vol. **10**, pp. 293–301
- [9] White W, Yu Z, Fateh F., 2015 Torsional resonance active damping in grid tied wind turbines with gearbox, DFIG, and power converters *American Control Conference, Chicago, 1-3 July*
- [10] Moriarty P, Hansen A, 2005 AeroDyn theory manual *NREL/TP-500-36881*
- [11] Jonkman J, Butterfield S, Musial W, Scott G 2009 Definition of a 5-MW reference wind turbine for offshore system development *NREL/TP-500-38060*
- [12] Girsang I, Dhupia J, Muljadi E, Singh M, Pao L 2014 Gearbox and Drivetrain Models to Study Dynamic Effects of Modern Wind Turbines *IEEE Transactions on Industry Applications* vol. **50** pp 3777-3786
- [13] Dempewolf K 2013 *Modellierung des dynamischen Verhaltens permanentmagneterregter Synchronmaschinen* Ph.D.-thesis (Hannover, Germany) pp 91-95
- [14] Infineon 2013 Technical information - IGBT-modules – FF650R17IE revision 3.3
- [15] Wintrich A, Nicolai U, Tursky W, Reimann T 2015 Application manual – power semiconductors *Online: <http://www.semikron.com/dl/service-support/downloads/download/semikron-application-manual-power-semiconductors-english-en-2015.pdf>*
- [16] ASTM E1049-85(2011)e1: Standard Practices for Cycle Counting in Fatigue Analysis 2011 ASTM International (Pennsylvania, USA)
- [17] Held M, Jacob P, Nicoletti G, Scacco P. and Poech M-H 1997 Fast Power Cycling Test for IGBT Modules in Traction Application *Second International Conference on Power Electronics and Drive Systems* (Singapore)
- [18] Mandic G, Nasiri A, Muljadi E, Oyague F 2012 Active torque control for gearbox load reduction in a variable-speed wind turbine *IEEE Transaction on Industry Applications* vol. **48**